DALTON
FULL PAPER

The effects of distal ligand substitution on the copper(II)/*bis*-(2,6-dipyrazol-1-ylpyridine) centre †

Nayan K. Solanki,[a] Michael A. Leech,[b] Eric J. L. McInnes,[c] Jing P. Zhao,[c] Frank E. Mabbs,[c] Neil Feeder,[a] Judith A. K. Howard,[b] John E. Davies,[a] Jeremy M. Rawson[a] and Malcolm A. Halcrow*[d]

[a] *Department of Chemistry, University of Cambridge, Lensfield Road, Cambridge, UK CB2 1EW*
[b] *Department of Chemistry, University of Durham, South Road, Durham, UK DH1 3LE*
[c] *CW EPR Service Centre, Department of Chemistry, University of Manchester, Oxford Road, Manchester, UK M13 9PL*
[d] *School of Chemistry, University of Leeds, Woodhouse Lane, Leeds, UK LS2 9JT. E-mail: M.A.Halcrow@chem.leeds.ac.uk*

Received 6th April 2001, Accepted 30th May 2001
First published as an Advance Article on the web 3rd July 2001

The complex $[Cu(L^4)_2](BF_4)_2$ (**3**; L^4 = 2-[pyrazol-1-yl]-6-[3-{2,4,6-trimethylphenyl}pyrazol-1-yl]pyridine) has been synthesised. Complex **3** crystallises in two crystal forms from $MeNO_2/Et_2O$. The monoclinic α-form contains crystallographically ordered, pseudo-Jahn–Teller elongated $\{d_{x^2-z^2}\}^1$ Cu(II) ions that are structurally very similar to $[Cu(L^2)_2](BF_4)_2$ (**1**; L^2 = 2,6-dipyrazol-1-ylpyridine). The Cu ion in the orthorhombic β-polymorph at 180 K exhibits Cu–N bond lengths that are rather different from the α-form, and which could correspond to a disordered $\{d_{x^2-z^2}\}^1$ Cu(II) centre; or, to a static, rhombically compressed ion with a $\{d_{z^2}\}^1$ ground state. Variable temperature EPR data favour the former interpretation. A crystal structure at 31 K of $[Cu(L^3)_2](BF_4)_2$ (**2**; L^3 = 2,6-bis-[3-{2,4,6-trimethylphenyl}pyrazol-1-yl]pyridine), a genuine $\{d_{z^2}\}^1$ ion, is also described. Comparison of the crystallographic data of **1**–**3** shows that the $\{d_{x^2-z^2}\}^1$-to-$\{d_{z^2}\}^1$ ground state change occurs concomitantly with only a small *z*-axis compression.

Introduction

In common with the stereochemically similar complexes $[Cu(terpy)_2]X_2$ ($X^- = Br^-$, PF_6^-),[1] $[Cu(dien)_2](NO_3)_2$[2] and $[Cu(L^1R)_2](BF_4)_2$ (R = Me, Cy),[3] $[Cu(L^2)_2](BF_4)_2$ (**1**) adopts a $\{d_{x^2-z^2}\}^1$ electronic ground state in the solid state and in solution (Scheme 1).[4,5] This corresponds structurally to a pseudo-Jahn–Teller elongation of the molecular *x*-axis.[4,6] In solid **1**, this structural elongation is dynamically disordered over the molecular *x*- and *y*-axes, which results in unique thermally induced Jahn–Teller switching behaviour involving a crystal phase change at 41 K.[6] We have shown that ligand substitution adjacent to the distal, pyrazole N-donors results in a change in electronic ground state in $[Cu(L^3)_2](ClO_4)_2$ (**2**), which adopts an unusual $\{d_{z^2}\}^1$ ground state in the solid and solution phases.[4,5] Although on symmetry grounds the Jahn–Teller theorem does not apply to **2**, this complex should still exhibit an axial or rhombic structural compression along the molecular *z*-axis (Scheme 1). This result is significant because, prior to our work, there was only one authenticated, homoleptic six-coordinate Cu(II) compound that exhibits a compressed molecular structure,[7,8] namely the 1-D coordination polymer $KAlCuF_6$;[9] some other Cu-doped lattices also exhibit this property.[10] Hence, it is clearly of interest to define the spectroscopic and structural properties of the near-homoleptic $\{d_{z^2}\}^1$ species **2**.

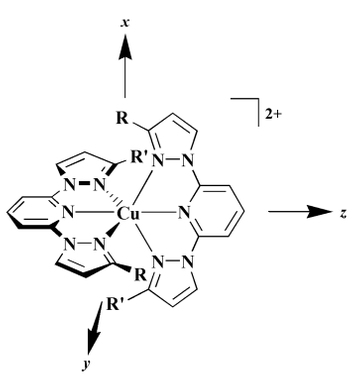

1 R = R' = H
2 R = R' = Mes
3 R = H, R' = Mes

Scheme 1 Molecular axes for $[CuL_2]^{2+}$ (L = L^2–L^4).

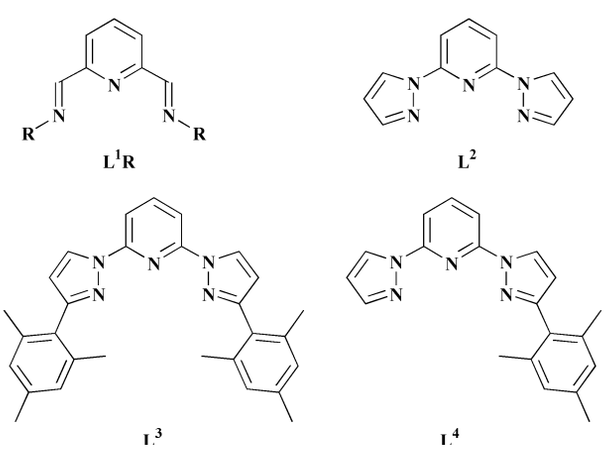

In order to examine further the steric factors that contribute towards the $\{d_{z^2}\}^1$ ground state of **2**, we have now prepared $[Cu(L^4)_2](ClO_4)_2$ (**3**). We report here variable temperature EPR

† *Non-SI unit employed*: 1 G = 10^{-4} T.

DOI: 10.1039/b103142m

and crystallographic studies of this complex, which define its electronic ground state. A low temperature X-ray structure determination of **2**[4] is also described. These results now allow us to elucidate changes in the molecular structure of this Cu(II) center that occur concomitantly with the change in ground state from $\{d_{y^2-z^2}\}^1$ to $\{d_{z^2}\}^1$. The molecular axis convention shown in Scheme 1 is used for the rhombic complexes described in this paper, with the short, intermediate and long Cu–N bonds being defined as lying near the molecular *z*-, *y*- and *x*-axes respectively.

Results and discussion

The new ligand L^4 was prepared by the sequential coupling of 2,6-dibromopyridine with one molar equivalent of potassium pyrazolide, followed by one molar equivalent of potassium 3{5}-(2,4,6-trimethylphenyl)pyrazolide, according to the method of Jameson and Goldsby.[11] Complexation of $Cu(ClO_4)_2\cdot 6H_2O$ by 2 molar equivalents of L^4 in $MeNO_2$ yields a lime green solution, from which feathery green microcrystals were obtained in good yield following concentration of the solution and addition of Et_2O. The dried solid analysed cleanly as the desired product $[Cu(L^4)_2](ClO_4)_2$ (**3**), a formulation confirmed by positive ion FAB mass spectrometry (*m*/*z* = 722, corresponding to $[^{63}Cu(L^4)_2 + H]^+$) and IR spectroscopy, which showed the presence of L^4 and ClO_4^- only. The d–d maxima exhibited by **3** in MeCN [$\nu_{max} = 6.0 \times 10^3$ cm^{-1} ($\varepsilon_{max} = 35$ M^{-1} cm^{-1}), 13.5 (48), 23.5 (108)] are very similar to those shown by **1** [6.3 (33), 13.9 (46), 24.4 (119)] and **2** [5.9 (44), 13.8 (52), 23.5 (sh)].[4]

Complex **3** is difficult to crystallise. However, diffusion of Et_2O vapor into a small volume (*ca.* 0.3 cm^3) of a solution of **3** in $MeNO_2$ sometimes yielded clusters of green needles, from which fragments suitable for X-ray analysis could be cleaved. Examination of several crystals from different samples obtained in this way revealed the presence of two solvated modifications: monoclinic $[Cu(L^4)_2](ClO_4)_2\cdot 2CH_3NO_2$ (α-**3**·$2CH_3NO_2$) and orthorhombic $[Cu(L^4)_2](ClO_4)_2\cdot x CH_3NO_2$ (β-**3**·$x CH_3NO_2$; $x \approx 2.0$). The uncertain composition of the β-polymorph reflects severe solvent disorder in this form (see below). Under the microscope, needles of the α-modification have a flatter cross-section compared to the β-polymorph, although they are indistinguishable to the naked eye.

Crystals of α-**3**·$2CH_3NO_2$ contain one cation, two anions and two fully occupied solvent sites per asymmetric unit, all lying on general positions. The six-coordinate complex at 150 K has a distribution of bond lengths that clearly arises from a crystallographically ordered Jahn–Teller elongated dication, the axis of elongation lying along the N(5)–Cu(1)–N(6) vector (Table 1, Fig. 1). At 30 K, the molecular structure of the complex is almost identical to that at 150 K, consistent with its being non-fluxional in the crystal. Interestingly, the distance Cu(1)–N(5) has lengthened slightly at 30 K, from 2.258(2) Å at 150 K to 2.2741(14) Å; the reason for this is uncertain. All other metric parameters at the Cu ion are crystallographically indistinguishable at the two temperatures. The Cu–N distances and N–Cu–N angles in α-**3**·$2CH_3NO_2$ resemble those in the low-temperature phase of **1** (Table 1).[6] The only manifestation of steric repulsion between the 2,4,6-trimethylphenyl substituents of one L^4 ligand in **3** and the pyridine ring of the other, is a slight elongation of the bonds Cu(1)–N(2) and Cu(1)–N(3) in **3**, which at 30 K are 0.029(2)–0.037(2) Å longer than the equivalent bonds in **1** at 31 K.

The structure of β-**3**·$x CH_3NO_2$ suffers badly from twinning problems, and from static anion and solvent disorder that reflects the presence of channels of solvent molecules within the crystal lattice, running parallel to the unit cell *c*-vector. Following unsuccessful attempts to collect data from several different crystals at several temperatures, we were able to obtain one useful refinement of this polymorph at 180 K. The Cu(II) ion in this modification at 180 K is also six-coordinate, but with Cu–N distances that differ significantly from those of α-**3**·$2CH_3NO_2$ (Table 1). Rather, the coordination sphere in this structure more closely resembles that of **2** (see below).[7] In principle, this could reflect the presence of either: a dynamically or statically disordered pseudo-Jahn–Teller elongated Cu(II) ion with a $\{d_{y^2-z^2}\}^1$ ground state; or a rhombically compressed Cu(II) centre analogous to **2**, with a $\{d_{z^2}\}^1$ ground state.[8,12]

In order to address this ambiguity, the vibrational amplitudes $\langle d^2 \rangle$ were calculated for both polymorphs of **3**.[8] This parameter corresponds to the difference in the mean-square displacement parameters (MSDAs) of a given N atom and the Cu atom along their common vector (eqn. 1 and 2).

$$\text{MSDA} = \frac{\sum_{i=1}^{3}\sum_{j=1}^{3} U_{ij} n_i n_j}{|n|^2} \quad (1)$$

$$\langle d^2 \rangle = \text{MSDA(N)} - \text{MSDA(Cu)} \quad (2)$$

Table 1 Selected bond lengths (Å) and angles (°) for α-$[Cu(L^4)_2](ClO_4)_2\cdot 2CH_3NO_2$ (α-**3**·$2CH_3NO_2$) and β-$[Cu(L^4)_2](ClO_4)_2\cdot x CH_3NO_2$ (β-**3**·$x CH_3NO_2$)

	α-**3**·$2CH_3NO_2$		β-**3**·$x CH_3NO_2$
	150 K	30 K	180 K
Cu–N(1)	1.962(2)	1.9668(14)	1.985(4)
Cu–N(2)	2.089(2)	2.0928(14)	2.173(4)
Cu–N(3)	2.101(2)	2.1012(14)	2.150(4)
Cu–N(4)	2.023(2)	2.0343(14)	1.996(4)
Cu–N(5)	2.258(2)	2.2741(14)	2.186(4)
Cu–N(6)	2.301(2)	2.3048(13)	2.220(4)
N(1)–Cu–N(2)	77.98(9)	78.10(5)	77.32(16)
N(1)–Cu–N(3)	78.04(9)	78.08(5)	76.99(16)
N(1)–Cu–N(4)	179.48(9)	176.22(5)	175.95(16)
N(1)–Cu–N(5)	108.62(9)	107.75(5)	107.65(15)
N(1)–Cu–N(6)	101.37(9)	102.36(5)	99.85(15)
N(2)–Cu–N(3)	155.81(9)	156.01(5)	153.65(16)
N(2)–Cu–N(4)	103.33(9)	103.48(5)	102.51(15)
N(2)–Cu–N(5)	93.89(9)	93.78(5)	91.98(15)
N(2)–Cu–N(6)	88.28(9)	88.54(5)	92.46(14)
N(3)–Cu–N(4)	100.82(9)	100.47(5)	103.53(16)
N(3)–Cu–N(5)	90.74(9)	90.80(5)	90.24(17)
N(3)–Cu–N(6)	99.53(9)	99.26(5)	97.59(16)
N(4)–Cu–N(5)	75.70(9)	75.67(5)	76.39(16)
N(4)–Cu–N(6)	74.43(9)	74.34(5)	76.11(15)
N(5)–Cu–N(6)	149.73(9)	149.63(5)	152.46(15)

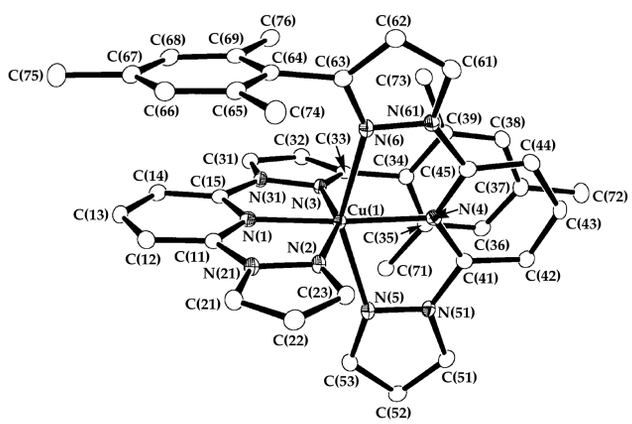

Fig. 1 View of the $[Cu(L^4)_2]^{2+}$ complex dication in the crystal of α-**3**·$2CH_3NO_2$ at 31 K, showing the atom numbering scheme adopted. The structure of the complex dication in β-**3**·$x CH_3NO_2$ is visually almost identical to that shown here, and uses the same atom numbering scheme. Thermal ellipsoids are at the 50% probability level, while all non-H atoms have been omitted for clarity.

Table 2 Calculated $\langle d^2 \rangle$ (10^4 Å^2) values for **2** and **3**. A negative value of $\langle d^2 \rangle$ arises when MDSA(N) < MDSA(Cu). Estimated errors on $\langle d^2 \rangle$ are $\pm 20 \times 10^4$ Å^2

	T/K	Cu(1)–N(1)	Cu(1)–N(2)	Cu(1)–N(3)	Cu(1)–N(4)	Cu(1)–N(5)	Cu(1)–N(6)
2	150[a]	−95	8	34	−69	18	15
	31	24	31	40	23	31	38
3, α-polymorph	150	24	62	−1	16	34	−16
	31	33	47	42	33	37	29
3, β-polymorph	180	−14	65	101	7	80	−40

[a] Taken from ref. 4.

where U_{ij} is an element of the 3×3 matrix of thermal parameters and n_i, n_j are elements of the vector describing the bond. It has been suggested that statically or dynamically disordered Cu–N bonds generally exhibit $\langle d^2 \rangle > 0.010$ Å^2, while ordered N-donor atoms afford $\langle d^2 \rangle$ values that are smaller than this value.[13] However, care must be taken using this criterion, since $\langle d^2 \rangle$ for fluxional Cu–X (X = N, O) bonds decreases markedly with decreasing temperature.[13,14] In our experience, this can lead to Cu–N bonds that (from variable temperature crystallography) are clearly dynamically disordered, but which show $\langle d^2 \rangle < 0.010$ Å^2 at lower temperatures.[15] All the $\langle d^2 \rangle$ values for the Cu–N bonds in β-**3**·$x$$CH_3NO_2$ are somewhat greater than for the α-polymorph, although only for the bond Cu(1)–N(3) in the β-form is $\langle d^2 \rangle$ greater than the putative 0.010 Å^2 threshold value (Table 2). Overall, these data are inconclusive; however, they do not rule out a dynamic $\{d_{y^2-z^2}\}^1$ ground state for β-**3**·$x$$CH_3NO_2$ (see below). A possible alternative explanation for the different Cu–N distances in the polymorphs of **3** might be the presence of a cocrystallised impurity in the β-form. However, no residual electron density that might arise from such a contaminant was detected in the Fourier map for this structure, while the displacement ellipsoids of all the atoms in the $[Cu(L^4)_2]^{2+}$ dication are consistent with it being fully crystallographically occupied.

Powder EPR spectra of **3** were obtained at Q-band over the range 5–296 K, using a mixture of the two polymorphs of this compound (see above). At all temperatures, the spectra could only be simulated assuming the presence of two distinct spin systems, populated in a ratio of approximately 3 : 1 which did not vary detectably with temperature (Table 3, Fig. 2). The major species has the form of a resolved molecular spectrum, with a rhombic $g_1 > g_2 \approx g_3 > g_e$ pattern and $A_1\{^{63,65}Cu\}$ coupling that are clearly consistent with a $\{d_{y^2-z^2}\}^1$ ground state.[16] The rhombicity of this signal decreases slightly as the temperature is lowered. However, the observed g-values are clearly consistent with this species having a static, rather than fluxional, axis of pseudo-Jahn–Teller elongation. The minor spin is apparently axial at 290 K with an 'inverse' $g_\perp > g_\parallel > g_e$ pattern. The g-values of this minor signal do not vary significantly with temperature until below 20 K. However, at 10 K this signal has changed substantially, to a rhombic $g_1 > g_2 > g_3 > g_e$ pattern (Fig. 2). This is the behaviour expected for an exchange-averaged spectrum, reflecting the fluxionality of a pseudo-Jahn–Teller axis of elongation (as in **1**).[1–3,8,12] The lack of observable hyperfine coupling in the minor spectrum is also consistent with this interpretation. The alternative description of this species, as a static $\{d_{z^2}\}^1$ species analogous to **2**, is ruled out because of the variation of this spectrum at low temperatures, and because $g_3 > g_e$.

It is clear from these measurements that solid **3** contains a mixture of static and fluxional $\{d_{y^2-z^2}\}^1$ spins. This is consistent with the observation of a static, rhombically elongated molecular structure in the α-**3**·2CH_3NO_2 modification and a potentially fluxional Cu(II) centre in β-**3**·$x$$CH_3NO_2$. The assignment of β-**3**·$x$$CH_3NO_2$ as a dynamic $\{d_{y^2-z^2}\}^1$ Cu(II) compound is not inconsistent with the crystallographic MSDA data for this polymorph (Table 2; see above). However, it would require a variable temperature crystallographic study to confirm this suggestion, which we have not yet been able to achieve. In frozen 10 : 1 MeCN–toluene solution, the same sample of **3** yields a single EPR peak, which resembles the major signal from the powder spectrum and is assignable to a pseudo-Jahn-Teller elongated $\{d_{y^2-z^2}\}^1$ Cu(II) ion (Table 3).[16]

Table 3 Q-Band EPR data for solid **3**. Hyperfine couplings are to ^{63,65}Cu and are in G. Estimated errors in g are ±0.002 for the major spin, and ±0.005 for the minor spin. Estimated errors in A are ±3 G

	Major species				Minor species		
T/K	g_1	g_2	g_3	A_1	g_1	g_2	g_3
296	2.280	2.116	2.050	130	2.200	2.200	2.050
220	2.286	2.106	2.050	130	2.200	2.200	2.050
180	2.290	2.100	2.050	130	2.200	2.200	2.020
80	2.296	2.092	2.050	135	2.200	2.200	2.020
40	2.296	2.089	2.058	135	2.200	2.200	2.020
20	2.296	2.087	2.058	135	2.200	2.200	2.020
10	2.298	2.087	2.057	135	2.250	2.116	2.030
5	2.300	2.087	2.057	135	2.250	2.126	2.030
120[a]	2.281	2.099	2.051	137	—	—	—

[a] Solution spectrum run in 10 : 1 MeCN–toluene.

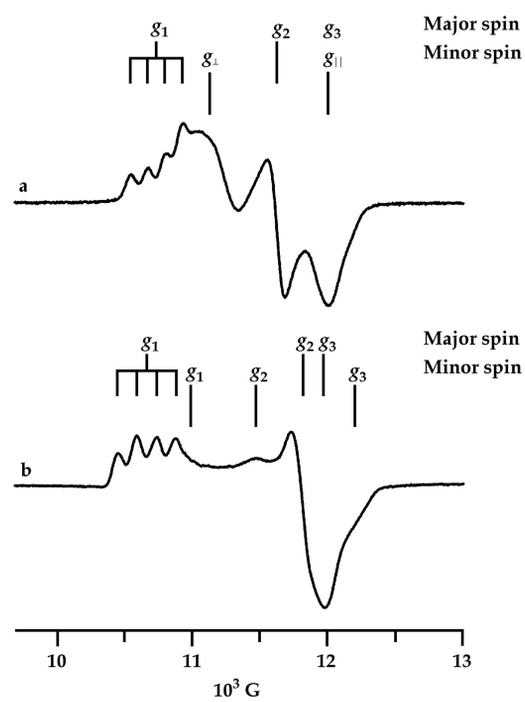

Fig. 2 Q-Band EPR spectra of powdered **3** at (a) 290 and (b) 5 K.

For comparison, a structure determination of **2**·2CH_3NO_2 was carried out at 31 K (Table 4, Fig. 3). All bond lengths and angles to copper in this structure are crystallographically identical to those we have previously reported for this compound at 180 K.[4] In addition, all the Cu–N bonds in **2** at both temperatures give $\langle d^2 \rangle < 0.010$ Å^2 (Table 2). These data

Table 4 Selected bond lengths (Å) and angles (°) for $[Cu(L^3)_2](ClO_4)_2 \cdot 2CH_3NO_2$ ($2 \cdot 2CH_3NO_2$) at 31 K

Cu–N(1)	1.9586(14)
Cu–N(2)	2.1371(14)
Cu–N(3)	2.1463(14)
Cu–N(4)	1.9799(14)
Cu–N(5)	2.2117(15)
Cu–N(6)	2.2503(15)
N(1)–Cu–N(2)	78.00(6)
N(1)–Cu–N(3)	78.14(6)
N(1)–Cu–N(4)	179.46(6)
N(1)–Cu–N(5)	103.44(5)
N(1)–Cu–N(6)	102.70(5)
N(2)–Cu–N(3)	156.08(5)
N(2)–Cu–N(4)	101.51(5)
N(2)–Cu–N(5)	95.38(5)
N(2)–Cu–N(6)	91.08(5)
N(3)–Cu–N(4)	102.34(5)
N(3)–Cu–N(5)	91.78(5)
N(3)–Cu–N(6)	92.47(5)
N(4)–Cu–N(5)	76.82(5)
N(4)–Cu–N(6)	77.05(5)
N(5)–Cu–N(6)	153.84(5)

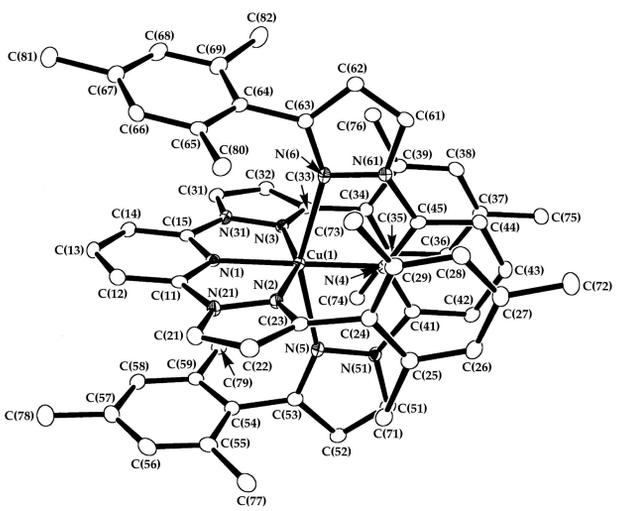

Fig. 3 View of the $[Cu(L^3)_2]^{2+}$ complex dication in the crystal of $2 \cdot 2CH_3NO_2$ at 31 K, showing the atom numbering scheme adopted. Details as for Fig. 1.

confirm our earlier conclusion that **2** is not fluxional in the solid state.

Concluding remarks

In order to determine the structural effects of the unusual electronic ground state in **2**, the most instructive comparison is between $2 \cdot 2CH_3NO_2$ and the α-modification of $3 \cdot 2CH_3NO_2$ at 31 K, since the latter will have a steric environment that most closely resembles that of **2**. For ease of comparison, the numbering scheme for the Cu and N atoms in these two structures is identical (Figs. 1 and 3). The two Cu–N bonds close to the molecular *y*-axis (Scheme 1) in **2**, Cu(1)–N(2) and Cu(1)–N(3), are each longer compared to those in **3** by 0.045(2) Å. The two *x*-axis Cu–N bonds in **2** are correspondingly shorter than in **3**, by 0.055(2) Å for Cu(1)–N(5) and 0.062(2) Å for Cu(1)–N(6). Hence, it is apparent that the change from a $\{d_{y^2}\}^1$ to a $\{d_{z^2}\}^1$ ground state in $[CuL_2]^{2+}$ (L = L^3, L^4) is reflected in a convergence of the Cu–N bond lengths along the molecular *x*- and *y*-axes, by roughly equivalent amounts.

Other things being equal, lengthening of the distal M–N bonds to a meridional tridentate ligand generally results in a concomitant elongation of the central M–N bond.[3] Hence, quantifying the behaviour of Cu–N bonds parallel to the molecular *z*-axis upon changing the Cu ion ground state is more difficult, because these will be dictated by conformational strain within the tridentate ligand as well as by the electronic configuration at Cu. The bonds Cu(1)–N(1) and Cu(1)–N(4) are both shorter in **3** than in **2**. However, the contraction of Cu(1)–N(1) [0.008(2) Å] is much smaller than for Cu(1)–N(4) [0.054(2) Å], because for the former bond ligand conformational effects will oppose the electronically imposed *z*-axis compression in **3** compared to **2**, while for Cu(1)–N(4) they will reinforce it. Taking an average of these two values to cancel the ligand conformational strain, it can be said that the $\{d_{y^2-z^2}\}^1$–$\{d_{z^2}\}^1$ transition occurs concomitantly with a 0.031(3) Å shortening of the two *z*-axis Cu–N bonds, which is somewhat smaller than the structural changes in the *xy*-plane.

A similar comparison between the structures of **1**[6] and **2** at 31 K leads to an identical trend to that described above. The more rhombic stereochemistry of **1** means that the changes in Cu–N bond length close to the *x*- and *y*-axes between **1** and **2** are greater compared to between **2** and **3**. Interestingly, however, the two pairs of compounds give rise to similar estimated *z*-axis contractions, of 0.025–0.030 Å. We have also reported a similar, but again more pronounced, trend between the structures of the $\{d_{y^2-z^2}\}^1$ complex $[Cu(L^1Cy)_2](BF_4)_2$, and the $\{d_{z^2}\}^1$ $[Cu(L^1Bu^t)_2](BF_4)_2$.[3] Hence, on the basis of this study and the work in ref. 3, it can be concluded that the structural distortion arising from a $\{d_{z^2}\}^1$ configuration in $[CuL_2]^{2+}$ (L = meridional tris-imine ligand) complexes is probably best considered as an elongation of the Cu–N bonds within the molecular *xy*-plane, rather than as a *z*-axis compression.

Experimental

Unless stated otherwise, all manipulations were performed in air. 2-Pyrazol-1-yl-6-bromopyridine,[11] 3{5}-(2,4,6-trimethylphenyl)pyrazole,[17] **1** and **2** were prepared by the literature procedures.[4] KH (35 wt% suspension in mineral oil, Aldrich) was washed twice with freshly distilled n-hexane under N_2, and dried *in vacuo*, before use. $Cu(ClO_4)_2 \cdot 6H_2O$ (Avocado) and all other solvents (analytical grade) were used as supplied, except that diglyme was dried over sodium before use.

Syntheses

2-(Pyrazol-1-yl)-6-(3-{2,4,6-trimethylphenyl}pyrazol-1-yl)-pyridine (L^4). To a suspension of KH (1.0 g, 2.6×10^{-2} mol) in diglyme (80 cm^3) under N_2 was added 3{5}-(2,4,6-trimethylphenyl)pyrazole (4.8 g, 2.6×10^{-2} mol), resulting in the vigorous evolution of H_2. The mixture was stirred for 1 h at 55 °C. 2-Pyrazol-1-yl-6-bromopyridine (5.7 g, 2.0×10^{-2} mol) was then added, and the resultant mixture stirred at 130 °C for 5 days. After cooling, an equal volume of water was added to the mixture, yielding an off-white precipitate, which was filtered and washed twice with water. Recrystallisation from CH_2Cl_2–MeOH yielded a pale yellow microcrystalline solid. Yield 2.9 g, 45% (Found: C, 72.7; H, 5.8; N, 20.9; calc. for $C_{20}H_{19}N_5$: C, 72.9; H, 5.8; N, 21.3%). Mp 140–142 °C. EI–MS: *m*/*z* 329 $[M]^+$, 185 [3{5}-mesitylpyrazole]$^+$, 145 [M − (3{5}-mesitylpyrazole) + H]$^+$. NMR ($CDCl_3$, 293K): ^{1}H, δ 8.64 (d, 2.2, 1H, Pz^{Mes} H^5), 8.61 (d, 2.3, 1H, Pz^H H^5), 7.83–7.92 (m, 3H, Py H^3–H^5), 7.78 (br s, 1H, Pz^H H^3), 6.97 (s, 2H, Ph $H^{3/5}$), 6.52 (br s, 1H, Pz^H H^4), 6.43 (d, 2.2 Hz, 1H, Pz^{Mes} H^4), 2.34 (s, 3H, CH_3), 2.21 (s, 6H, CH_3); ^{13}C, δ 153.8, 150.2, 150.1 (Py C^2 + Py C^6 + Pz^{Mes} C^3), 142.4, 141.4 (Pz^H C^3 + Py C^4), 137.9 (Ph C^1), 137.4 (Ph $C^{2/6}$), 130.3 (Ph C^4), 128.3 (Ph $C^{3/5}$), 127.3, 127.0 ($Pz^H C^5$ + Pz^{Mes} C^5), 109.5, 109.5 (Py C^3 + Py C^5), 109.0, 108.0 (Pz^H C^4 + Pz^{Mes} C^4), 21.1 (Mes CH_3), 20.6 (Mes CH_3).

Bis-[2-(pyrazol-1-yl)-6-(3-{2,4,6-trimethylphenyl}pyrazol-1-yl)pyridine]copper(II) diperchlorate (3). A solution of L^4 (0.80 g, 2.4×10^{-3} mol) and $Cu(ClO_4)_2 \cdot 6H_2O$ (0.44 g, 1.2×10^{-3} mol) in $MeNO_2$ (30 cm^3) was stirred for 10 min at room temperature.

Table 5 Experimental details for the single crystal structure determinations in this study

	$[Cu(L^3)_2](ClO_4)_2\cdot 2CH_3NO_2$ (**2**·$2CH_3NO_2$)	α-$[Cu(L^4)_2](ClO_4)_2\cdot 2CH_3NO_2$ (α-**3**·$2CH_3NO_2$)	α-$[Cu(L^4)_2](ClO_4)_2\cdot 2CH_3NO_2$ (α-**3**·$2CH_3NO_2$)	β-$[Cu(L^4)_2](ClO_4)_2\cdot 2.5CH_3NO_2$ (β-**3**·$2.0CH_3NO_2$)
Formula	$C_{60}H_{64}Cl_2CuN_{12}O_{12}$	$C_{42}H_{44}Cl_2CuN_{12}O_{12}$	$C_{42}H_{44}Cl_2CuN_{12}O_{12}$	$C_{60}H_{64}Cl_2CuN_{12}O_{12}$
M_r	1279.67	1043.33	1043.33	1279.67
T/K	31(2)	150(2)	30(2)	180(2)
Crystal class	Monoclinic	Monoclinic	Monoclinic	Orthorhombic
Space group	$P2_1/c$	$P2_1/c$	$P2_1/c$	$Pbcn$
a/Å	12.0031(15)	18.6594(6)	18.5980(13)	40.780(6)
b/Å	19.684(2)	18.1992(6)	18.2528(12)	18.023(3)
c/Å	24.967(3)	14.8395(4)	14.6183(10)	13.673(3)
β/°	99.955(2)	111.396(2)	111.2280(10)	—
V/Å^3	5810.1(12)	4692.0(3)	4625.7(5)	5810.1(12)
Z	4	4	4	4
μ(Mo-Kα, mm^{-1})	0.543	0.654	0.663	0.543
Measured reflections	47634	24012	33683	16792
Independent reflections	12155	8214	9384	8872
R_{int}	0.038	0.061	0.029	0.044
$R(F)$[a]	0.032	0.047	0.030	0.089
$wR(F^2)$[b]	0.085	0.123	0.084	0.274

[a] $R = \Sigma[|F_o| - |F_c|]/\Sigma|F_o|$. [b] $wR = [\Sigma w(F_o^2 - F_c^2)/\Sigma wF_o^4]^{1/2}$.

The lime green solution was filtered and concentrated to *ca.* 5 cm^3. Vapor diffusion of Et_2O into this solution afforded feathery green microcrystals. Yield 0.97 g, 86% (Found: C, 52.1; H, 4.3; N, 15.2; calc. for $C_{40}H_{38}Cl_2CuN_{10}O_8$: C, 52.2; H, 4.2; N, 15.2%). FAB-MS: *m*/*z* 722 $[^{63}Cu(L^4)_2 + H]^+$, 392 $[^{63}Cu(L^4)]^+$, 330 $[L^4+H]^+$. UV/vis/NIR (CH_3CN): ν_{max} 10^3 cm^{-1} (ε_{max}, M^{-1} cm^{-1}) 6.0 (35), 13.5 (48), 23.5 (108), 30.1 (sh), 30.5 (27,800), 36.1 (sh), 36.8 (30,200), 40.5 (sh), 43.4 (sh), 44.8 (sh).

CAUTION: although we have experienced no difficulties in handling **3**, metal-organic perchlorates are potentially explosive and should only be prepared or manipulated in small quantities.

Single crystal X-ray structure determinations

Single crystals of **2** and **3** were grown by vapour diffusion of Et_2O into solutions of the complexes in $MeNO_2$. Experimental details from the structure determinations are given in Table 5. All X-ray data at 31 K were obtained using a Siemens SMART diffractometer fitted with an Oxford Cryosystems HELIX helium cooling device. All measurements at temperatures equal to or above 100 K were collected using an Enraf Nonius KappaCCD diffractometer fitted with an Oxford Cryosystems nitrogen cooling device. Crystals were mounted on a glass ($T \geq 100$ K) or nylon ($T \leq 50$ K) fibre using a drop of perfluoropolyether oil. All structures were solved by direct methods (SHELXS 86[18]) and refined by full matrix least-squares on F^2 (SHELXL 97[19]), with H atoms placed in calculated positions. Mean-square diplacement parameters were calculated using the program THMA11,[20] incorporated into the WinGX suite of crystallographic software.[21]

CCDC reference numbers 164481–164484.

See http://www.rsc.org/suppdata/dt/b1/b103142m/ for crystallographic data in CIF or other electronic format.

$[Cu(L^3)_2](ClO_4)_2\cdot 2CH_3NO_2$ (2·$2CH_3NO_2$) at 31 K and α-$[Cu(L^4)_2](ClO_4)_2\cdot 2CH_3NO_2$ (α-3·$2CH_3NO_2$) at 30 K. No disorder was detected during refinement of either of these structures, and no restraints were applied to the final models. All non-H atoms were refined anisotropically.

α-$[Cu(L^4)_2](ClO_4)_2\cdot 2CH_3NO_2$ (α-3·$2CH_3NO_2$) at 150 K. One perchlorate anion was disordered over two distinct orientations, which were modeled with a 0.75 : 0.25 occupancy ratio. All Cl–O distances within the disordered anion were restrained to 1.41(2) Å, and non-bonded O···O distances within a particular disorder orientation to 2.27(2) Å. All non-H atoms except the minor anion disorder orientation were modeled anisotropically.

β-$[Cu(L^4)_2](ClO_4)_2\cdot x CH_3NO_2$ (β-3·$x CH_3NO_2$; $x \approx 2.0$) at 180 K. The lattice of this structure contains channels of solvent molecules running parallel to the *z*-axis of the unit cell, giving rise to substantial anion and solvent disorder. One perchlorate anion was disordered by rotation about one Cl–O bond, with the remaining three O atoms each being distributed over three equally occupied sites. The second anion was disordered over two sites, with a 0.7 : 0.3 occupancy ratio. All Cl–O distances within the disordered anion were restrained to 1.43(2) Å, and non-bonded O···O distances within a particular disorder orientation to 2.34(2) Å. Four different solvent molecules were refined: one wholly occupied ordered site lying across a crystallographic C_2 axis; one wholly occupied site, whose O atoms were disordered over two equally occupied orientations; one site with occupancy 0.75; and one with occupancy 0.25, with one O atom lying on a crystallographic C_2 axis. All N–O distances were restrained to 1.22(2) Å. All non-H atoms with occupancy ≥ 0.5 were modeled anisotropically.

Other measurements

Infrared spectra were obtained from Nujol mulls pressed between KBr plates, in the range 400–4000 cm^{-1} using a Perkin-Elmer Paragon 1000 spectrophotometer. UV/visible spectra were obtained with Perkin-Elmer Lambda 12 or Lambda 900 spectrophotometers, in 1 cm quartz cells. All NMR spectra were run on a Bruker ARX250 spectrometer, operating at 250.1 (^{1}H) and 62.9 MHz (^{13}C). Electron impact and positive ion fast atom bombardment mass spectra were performed on a Kratos MS890 spectrometer, the FAB spectra employing a 3-NOBA matrix. CHN microanalyses were performed by the University of Cambridge Department of Chemistry microanalytical service. Melting points are uncorrected. Q-Band EPR spectra were obtained using a Bruker ESP300E spectrometer, fitted with an ER5106QT resonator and ER4118VT cryostat. Spectral simulations were performed using in-house software which has been described elsewhere.[22]

Acknowledgements

Financial support is acknowledged from the Royal Society (London) for a research fellowship to M. A. H., the EPSRC (N. K. S., M. A. L.), ICI R&T Division (N. K. S.), the University of Cambridge and the University of Leeds.

References

1 J.-V. Folgado, W. Henke, R. Allmann, H. Stratemeier, D. Beltrán-Porter, T. Rojo and D. Reinen, *Inorg. Chem.*, 1990, **29**, 2035.
2 M. Duggan, B. J. Hathaway and J. Mullane, *J. Chem. Soc., Dalton Trans.*, 1980, 690.
3 J. M. Holland, X. Liu, J. P. Zhao, F. E. Mabbs, C. A. Kilner, M. Thornton-Pett and M. A. Halcrow, *J. Chem. Soc., Dalton Trans.*, 2000, 3316.
4 N. K. Solanki, E. J. L. McInnes, F. E. Mabbs, S. Radojevic, M. McPartlin, N. Feeder, J. E. Davies and M. A. Halcrow, *Angew. Chem., Int. Ed.*, 1998, **37**, 2221.
5 A. J. Bridgeman, M. A. Halcrow, M. Jones, E. Krausz and N. K. Solanki, *Chem. Phys. Lett.*, 1999, **314**, 176.
6 M. A. Leech, N. K. Solanki, M. A. Halcrow, J. A. K. Howard and S. Dahaoui, *Chem. Commun.*, 1999, 2245.
7 M. A. Hitchman, *Comments Inorg. Chem.*, 1994, **15**, 197.
8 L. R. Falvello, *J. Chem. Soc., Dalton Trans.*, 1997, 4463.
9 G. Wingefeld and R. Hoppe, *Z. Anorg. Allg. Chem.*, 1984, **516**, 223; K. Finnie, L. Dubicki, E. R. Krausz and M. J. Riley, *Inorg. Chem.*, 1990, **29**, 3908; M. Atanasov, M. A. Hitchman, R. Hoppe, K. S. Murray, B. Moubaraki, D. Reinen and H. Stratemeier, *Inorg. Chem.*, 1993, **32**, 3397; V. M. Masters, M. J. Riley and M. A. Hitchman, *J. Synchrotron Radiat.*, 1999, **6**, 242.
10 G. Steffen, D. Reinen, H. Stratemeier, M. J. Riley, M. A. Hitchman, H. Mathies, K. Recker, F. Wallrafen and J. R. Niklas, *Inorg. Chem.*, 1990, **29**, 2123; D. Reinen, G. Steffen, M. A. Hitchman, H. Stratemeier, L. Dubicki, E. R. Krausz, M. J. Riley, H. E. Mathies, K. Recker and F. Wallrafen, *Chem. Phys.*, 1991, **155**, 117.
11 D. L. Jameson and K. A. Goldsby, *J. Org. Chem.*, 1990, **55**, 4992.
12 D. Reinen and M. A. Hitchman, *Z. Phys. Chem.*, 1997, **200**, 11.
13 B. J. Hathaway, *Struct. Bonding (Berlin)*, 1984, **57**, 55.
14 C. J. Simmons, *New J. Chem.*, 1993, **17**, 77.
15 N. K. Solanki, M. A. Leech, E. J. L. McInnes, F. E. Mabbs, J. A. K. Howard, C. A. Kilner, M. Thornton-Pett, J. M. Rawson and M. A. Halcrow, unpublished work.
16 B. A. Goodman and J. B. Raynor, *Adv. Inorg. Chem.*, 1970, **13**, 135.
17 A. L. Rheingold, C. B. White and S. Trofimenko, *Inorg. Chem.*, 1993, **32**, 3471.
18 G. M. Sheldrick, *Acta Crystallogr., Sect. A*, 1990, **46**, 467.
19 G. M. Sheldrick SHELXL97, Program for the refinement of crystal structures, University of Göttingen, Germany, 1997.
20 J. D. Dunitz, V. Schomaker and K. N. Trueblood, *J. Chem. Phys.*, 1988, **92**, 856.
21 L. J. Farrugia, *J. Appl. Crystallogr.*, 1999, **32**, 837.
22 F. E. Mabbs and O. D. Collison, *Electron Paramagnetic Resonance of d Transition Metal Compounds*, Elsevier, Amsterdam, The Netherlands, 1992, ch. 7.